Electrochemical Monitoring of Cisplatin as Anticancer Compound to the Treatment of Laryngeal Cancer in the Elederly Using Poly(cyanocobalamin) Modified Composite of Ag Nanoparticles Graphene Oxide Electrode

Wei Ni, Qin Li, Yidao Jiang[*]

Otolaryngology Head and Neck Surgery, Jingzhou Central Hospital, Jingzhou, 434020, China
[*]Email: jyd18107167013@163.com

The purpose of this research was to develop a poly(cyanocobalamin) modified composite of Ag nanoparticles graphene oxide (poly(cyc)/Ag-GO) for electrochemical monitoring of cisplatin, a chemotherapy medication used to treat laryngeal cancer. The Ag-GO composite was electrodeposied on a glassy carbon electrode (GCE), and then poly(cyc) was electropolymerized on Ag-GO/GCE. The XRD and FE-SEM structural characterization of Ag-GO nanocomposite revealed that the Ag nanoparticles were discretely distributed on the surface of the GO nanosheets, resulting in a high porous structure with discrete electroactive sites for cyanocobalamin's strong bond and improved electron transfer and signal in electrochemical reactions. Using CV and DPV, electrochemical analyses revealed a stable, sensitive, and selective response of poly(cyc)/Ag-GO/GCE to cisplatin determination. The proposed sensor's detection limit, sensitivity, and linear range were determined to be 0.2 µM, 0.01316 µA/µM, and 40-1200 µM, respectively. The sensor's capability was tested using prepared platinol injection and human serum as real samples, and the results revealed acceptable recovery (95.25% to 98.50%) and RSD (3.08% to 4.76%), implying that the proposed cisplatin sensor is accurate enough for clinical sample analysis.

1. INTRODUCTION

Laryngeal cancer is a rare cancer in which malignant cells grow in the tissues of the larynx, or voice box [1]. It accounts for one-third of all head and neck cancers and may be a significant source of morbidity and mortality [2, 3]. Smoking tobacco, drinking alcohol, and human papillomavirus infections are the most important risk factors for laryngeal cancer [4, 5]. Signs and symptoms of

Int. J. Electrochem. Sci., 17 **(2022)** Article Number: 220124

2

laryngeal cancer include a sore throat and ear pain, a persistent cough, hoarseness, difficult or noisy breathing and difficulty or pain when swallowing [6, 7].

This type of cancer is rare among people under 40. It's more common in people in their 60s and 70s. Depending on the stage of the cancer, treatment can include surgery, radiation therapy and chemotherapy [8, 9]. Chemotherapy drugs for treating laryngeal cancer include cisplatin, fluorouracil, capecitabine, carboplatin, paclitaxel and gemcitabine [10]. Among these drugs, cisplatin as the most powerful and widely used treatment, has been shown to have satisfactory effects on advanced laryngeal cancer [11, 12].

As a cytotoxic agent in cancer cells, cisplatin ($Pt(NH_3)_2Cl_2$) can bind to nitrogen atoms of DNA bases and reactive centers on purine residues [13, 14]. It causes induced DNA interstrand crosslinking which can block the cell division and result in apoptotic cell death [15]. However, it has toxic side effects such as bruising and bleeding, anemia, renal vasoconstriction, and irreversible neurosensorial hearing loss and increased risk of infection due to a reduction in the number of white blood cells in blood. Moreover, cisplatin induces a cumulative dose-dependent axonal sensory neuropathy [16]. Therefore, various cisplatin doses have been incorporated into multiple treatment regimens.

A variety of analytical techniques such as high-performance liquid chromatographic assay [17], capillary electrophoresis [18], mass spectrometry [19], UV–vis spectrophotometry [20], atomic absorption spectrometry [21] and electrochemistry [22-26] have been applied for the determination of cisplatin in pharmaceutical specimens, biological fluids and tissues. Between them, electrochemical techniques have been found to exhibit significant advantages over other sensing technologies such as fast response, inexpensiveness, and simplicity [27]. In addition, the use of nanotechnology and various composites as surface modification technologies for electrodes in electrochemical cells has resulted in the highly sensitive and stable response of sensors [28, 29]. Therefore, this study was conducted on electrochemical monitoring of cisplatin using poly(cyc)/Ag-GO/GCE.

2. MATERIALS AND METHOD

2.1 Synthesis of poly(cyc)/Ag-GO/GCE

Before the modification, the GCE surface was polished with alumina powders (0.3 and 0.05 µm, Buehler Micropolish, USA) on a microcloth pad for 15 minutes. Then, the GCE was washed with a mixture of deionized water and ethanol (95%, Xinxiang XF Medical New Material Co., Ltd., China) using magnetic stirring for 10 minutes. After then, the electrode was rinsed with deionized water. For modification of the GCE using electrochemical deposition, the electrolyte was prepared from 8mM $AgNO_3$ (≥99.0%, Merck, Germany) and 2mg/ml GO (99%) in a 0.5M PBS solution pH 9.0. Deposition of Ag-GO nanocomposite on the GCE surface was performed on potentiostat/galvanostat system (CS310, Xian Yima Optoelec Co., Ltd., China) using a three-electrode setup including a GCE as the working electrode, a platinum wire as the counter electrode, and Ag/AgCl (3M KCl) as the reference electrode. This procedure was conducted in a potential range from -0.2 V to 1.3 V at a rate of 50 mV/s for 20 cycles under magnetic stirring [30]. For preparation the cyanocobalamin (cyc,≥98%, Sigma-Aldrich) modified electrode using the electro-polymerization in potentiostat/galvanostat system [31],

the polymertic films were deposited on GCE, GO/GCE, Ag/GCE and Ag-GO/GCE using CV technique at potential range from −1.2 V to 1.0 V a rate of 50 mV/s in a dimethylformamide (DMF, ,≥99%, Sigma-Aldrich) solution containing 2mM of cyanocobalamin and 0.1M $NaClO_4$ (≥98%, Sigma-Aldrich).

2.2. Preparation of Real samples

In order to prepare the pharmaceutical real samples of cisplatin, platinol injection (Teva Generics, USA) was used which contained 1 mg/ml of cisplatin. To prepare the 0.1 mg/ml of cisplatin solution in the electrochemical cell, the platinol was added to 0.1M PBS (pH=7.5) in a volume ratio of 1:9. To prepare a real sample of human serum, the cisplatin-free serum samples were provided by Peking University International Hospital (Beijing, China) which were diluted with the 0.1 M PBS in volume ratio of 1:10. For electrochemical analysis the DPV measurement was carried out in 0.1M PBS (pH=7.5) at a 10mV/s scan rate, and the standard addition system was used for analytical investigations of both real samples.

In order to further clinical investigation, the DPV measurements were carried out for determination of the cisplatin content in the urine of five patients aged 64 to 72 years with laryngeal cancer who underwent platinol injection treatment in Jingzhou Tumor Hospital (Jingzhou, Hubei, China). Accordingly, the urine samples were centrifuged at 1000 rpm for 10 minutes and the resultant supernatants were used to prepare 0.1M PBS (pH=7.5). Subsequently, the poly(cyc)/Ag-GO/GCE was used to determine the concentration of mifepristone in the prepared real samples using the DPV technique. Moreover, the urine samples were also analyzed with high-performance liquid chromatography-mass spectrometry (HPLC-MS). For preparation of the urine samples in the HPLC-MS system [32], 500 µl of urine samples were added into 100 µl of 5% diethyldithiocarbamate (99%, Sigma-Aldrich) solution, which was prepared in a 40g/l NaOH (99.99%, Merck, Germany) solution. Subsequently, the samples were homogenized by vortexing for 25 s and incubated for 15min at 40°C. Afterward, the samples were mixed with 1500 µl of acetonitrile (70%, Sigma-Aldrich). Then, the samples were homogenized by vortexing for 25s, and centrifuged at 2000 rpm for 15 min. 1.0µl of the resultant supernatants were injected into the HPLC-MS system where HPLC (1290 Infinity series Agilent Technologies, Santa Clara, CA, USA) combined with mass spectrometry (MS, Agilent 6230, Agilent Technologies, Germany) and was used to determine the presence of cisplatin in urine samples. Elution solvents were 0.1% formic acid (95%, Sigma-Aldrich) in acetonitrile and 0.1% formic acid in deionized water in gradient mode at a flow rate of 250 l/min in liquid chromatography (LC, ExtendC18 column 2.1×15 mm, 1.8 m, Agilent). The MS system was conducted in positive ionization mode, gas temperature of 320°C, an N_2 flow rate of 10 l/min, a nebulizer pressure of 40 psi, a capillary voltage of 3500 V, and an applied fragmentor voltage of 100 V.

2.3. Characterization

Electrochemical analyses were carried out using cyclic voltammetry (CV) and differential pulse voltammetry (DPV) techniques which were conducted on the potentiostat/galvanostat system in 0.1M

PBS (pH=7.5) which was prepared using a mixture of Na$_2$HPO$_4$ (99%, Merck, Germany).and NaH$_2$PO$_4$ (99%, Merck, Germany). X-ray diffraction (XRD; Rigaku D-max 2500 instrument, Japan) and field emission scanning electron microscopy (FE-SEM; JEOL JSM5410 instrument, Japan) analyses were performed for structural and morphological analyses of the nanostructure modified electrode.

3. RESULTS AND DISCUSSION

Figure 1 displays the FE-SEM micrographs of electrodeposited GO and Ag-GO on the GCE surface. The FE-SEM of GO reveals the exfoliated, crumpled, and wrinkled structure of GO nanosheets, and the generated porous and stacked framework of GO nanosheets provides good chemical catalysis and absorption sites [33, 34]. As seen from Figure 1b, the FE-SEM image of electrodeposited Ag-GO nanocomposite shows the Ag nanoparticles were discretely distributed on the surface of the GO nanosheets. The Ag nanoparticles were synthesized on GO nanosheets with an average diameter of 90nm. The results are evident that electrodepositition has a major role in the nucleation and growth of Ag nanoparticles on GO nanosheets which provide a high porous structure with the discrete electroactive sites and sharp tips for improving the electron transfer and signal in electrochemical reactions [35-37].
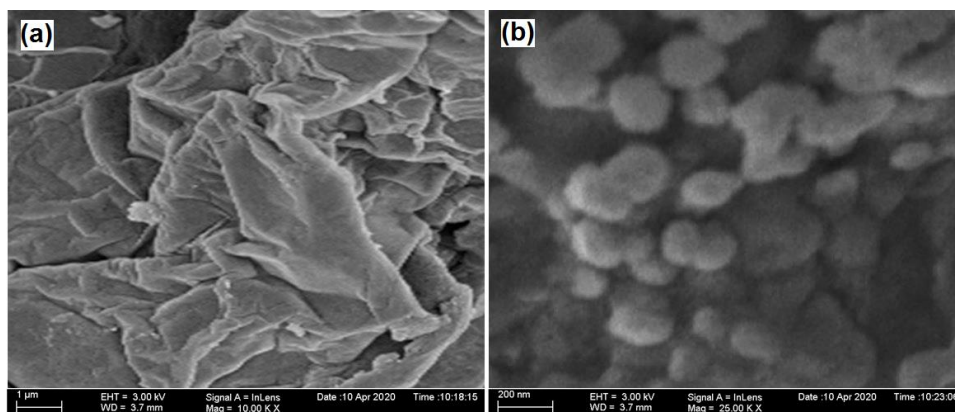

Figure 1. FE-SEM micrographs of electrodeposited (a) GO, (b) Ag-GO on GCE surface

Figure 2 shows the XRD patterns of powders of electrodeposited GO, Ag nanoparticles and Ag-GO on the GCE surface. XRD patterns of GO display a single sharp diffraction peak at 10.21° related to the (001) crystal plane of GO nanosheets [35]. In the XRD pattern of electrodeposited Ag nanoparticles Fig. 2b, the diffraction peaks are observed at 37.77°, 44.14°, 64.37°, and 77.42° which are attributed to the (111), (200), (220), and (311) planes of Ag nanoparticles that confirm the growth in the face-centered cubic (fcc) lattice (JCPDS card No. 04-783). The XRD patterns of Ag-GO in Fig. 2c reveal the (111), (200), (220), and (311) planes of fcc lattice Ag and (001) crystal plane of GO, indicating the simultaneous electrodeposition of GO nanosheets and Ag nanoparticles on the GCE surface and deposition of Ag nanoparticles on GO nanosheets which are in agreement with the FE-SEM results.
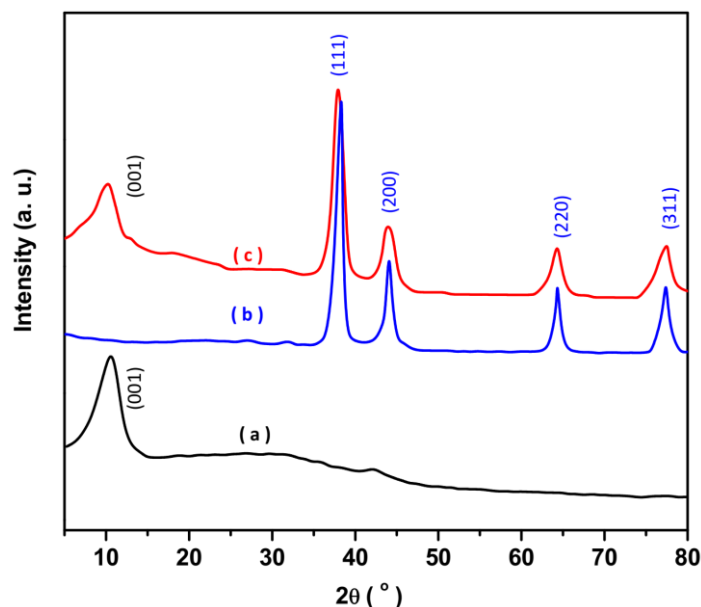
Figure 2. XRD pattern of powders of electrodeposited (a) GO, (b) Ag nanoparticles and (c) Ag-GO on GCE surface
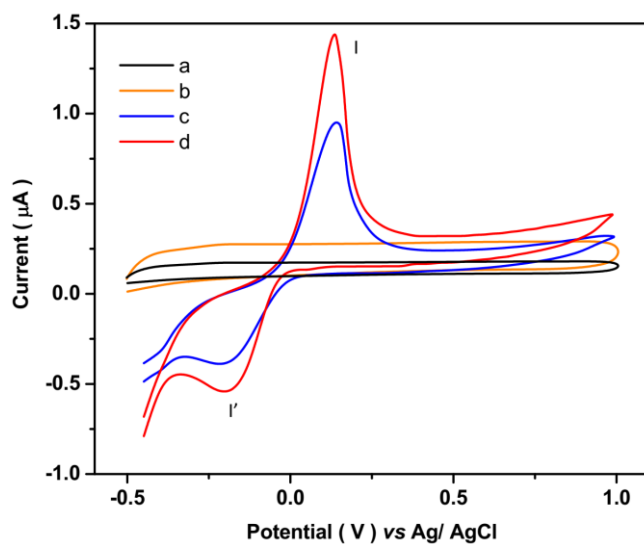

Figure 3. The electrochemical properties of (a) bare GCE, (b) GO/GCE, (c) Ag/GCE and (d) Ag-GO/GCE using CV experiments in 0.1M PBS (pH=7.5) at 10mV/s scan rate.

Figure 3 shows the electrochemical properties of bare GCE, GO/GCE, Ag/GCE and Ag-GO/GCE which were recorded using CV experiments in 0.1M PBS (pH=7.5) at 10mV/s scan rate. As observed from the CV curves in Figures 3a and 3b, GCE and GO/GCE do not show any redox peaks. On the contrary, after modification of the GCE surface with Ag nanoparticles and Ag-GO nanocomposite, the CV curves of Figures 3c and 3d shows the a prominent redox peak (I) at 0.13 V and –0.20 V (I') which is attributed to Ag oxidation (Ag^0 to Ag^+) and Ag^+ reduction (Ag^+ to Ag^0) [38], respectively. Comparison between the CV curves indicates using the GO matrix for modification of the electrodes surfaces enhances the electrochemical signal because of its great surface area, high

conductivity, durability, and numerous surface functional groups on nanosheets [39, 40]. Additionally, the presence of redox active Ag nanoparticles gives rise to an increase in electrical conductivity [41]. The simultaneous electrodeposition of GO nanosheets and Ag nanoparticles results in a high porous layer of Ag-GO nanocomposite on GCE, and small size of the electrodeposited nanoparticles leads to improved electron transfer and electrochemical current [42].

Moreover, the stability of the electrochemical response of modified poly(cyc) electrodes was investigated through the record of successive CVs in 0.1M PBS (pH=7.5) at a 10mV/s scan rate. It can be observed from Figure 4, first CV curves of poly(cyc) modified GCE, GO/GCE, Ag/GCE and Ag-GO/GCE show two reversible electron transfer processes, containing the two pairs of well-defined redox peaks at−0.83 V and −0.78 V (peaks II and II') and, -0.1V and 0.04 V (peaks III and III') which attributed to Co(III)/(II) and Co(II)/(I) redox process [31, 43], respectively. Moreover, the CV plots of poly(cyc)/Ag/GCE and poly(cyc)/Ag-GO/GCE show the Ag^0/Ag^+ redox peaks at 0.13 V (I) and –0.20 V (I'). The higher current peaks are belonging to poly(cyc)/Ag/GCE and poly(cyc)/Ag-GO/GCE. The 40th CV curves of poly(cyc) modified GCE, GO/GCE, Ag/GCE and Ag-GO/GCE show 30, 26, 15 and 5% decrease of redox peaks current, indicating poly(cyc)/GCE, poly(cyc)/GO/GCE and poly(cyc)/Ag/GCE exhibit the unstable response after several numbers of cycles, and the highest stability of electrochemical response of poly(cyc)/Ag-GO/GCE in 0.1M PBS (pH=7.5) that it may be due to the strong bond of cyanocobalamin on discrete electrodeposited Ag nanoparticles on GO [44, 45]. Therefore, among the modified poly(cyc) electrodes, the poly(cyc)/Ag-GO/GCE was chosen for further electrochemical studies.
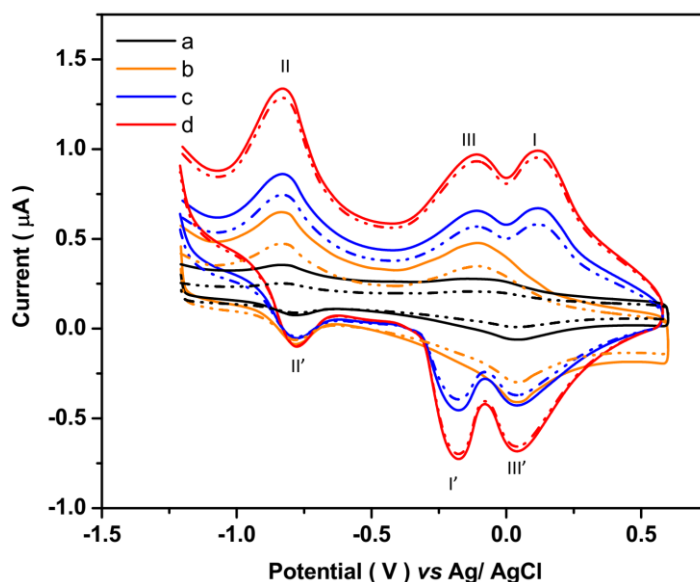

Figure 4. The first (solid line) and 40th (dashed line) CV plots of poly(cyc) modified (a) GCE, (b) GO/GCE, (c) Ag/GCE and (d) Ag-GO/GCE in 0.1 M PBS (pH 7.5) at scan rate of 10 mV/s.

Figure 5 depicts the DPV curves of bare GCE and modified GCE in 0.1M PBS (pH=7.5) at a 10mV/s scan rate in the presence of 40μM cisplatin solution. As seen, the DPV plots of GCE, GO/GCE, Ag/GCE, Ag-GO/GCE and poly(cyc)/Ag-GO/GCE exhibit the anodic peak of cisplatin at -

0.1V, which is correlated with the electrochemical oxidation of the reactive hydroxo complex of cis-$[Pt(H_2O)2(NH_3)_2]^{2+}$ of cisplatin [46]. Cisplatin chemistry in aqueous solution studies have shown that the chloro ligands of cisplatin can be replaced by the water molecule, forming cis-$[Pt(H_2O)2(NH_3)_2]^{2+}$ [47, 48]. Moreover, a very weak and broad oxidation peak is observed for bare GCE. The peak current and electron transport rate in poly(cyc)/Ag-GO/GCE were improved due to the nano-scale morphology of GO and Ag nanoparticles [49], and interaction between poly(cyc) and cisplatin [50, 51]. In addition, the synergetic effect of GO and Ag nanoparticles in Ag-GO/GCE forms the nanoporous structure and great effective surface area [50-53], and the interaction of cyanocobalamin with cisplatin promotes the accumulated amount of cisplatin [46], and enhances the sensitivity of the poly(cyc)/Ag-GO/GCE sensor. Therefore, the poly(cyc)/Ag-GO/GCE was used for the resultant electrochemical studies of cisplatin determination.
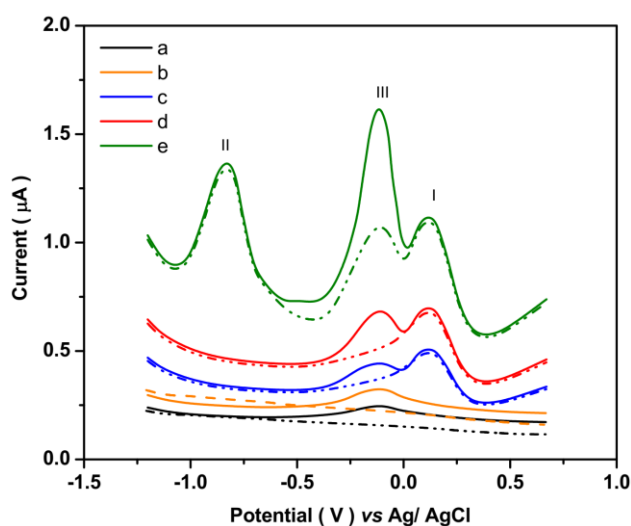

Figure 5. DPV plots of (a) GCE,(b) GO/GCE, (c) Ag/GCE, (d) Ag-GO/GCE and (e) poly(cyc)/Ag-GO/GCE into 0.1M PBS (pH=7.5) in 10mV/s scan rate in absence (dashed line) and presence (solid line) of 40μM cisplatin solution.

Figure 6 shows the results of a study of concentration effect of cisplatin on the electrochemical response of poly(cyc)/Ag-GO/GCE in 0.1M PBS (pH=7.5) at a 10mV/s scan rate. As observed from DPV curves in Figure 6a, the oxidation peak current of cisplatin at -0.1V is linearly improved with the successive addition of 40 μM cisplatin in the electrochemical cell. The obtained calibration plots in Figure 6b reveal that the limit of detection and the sensitivity of the proposed sensor for determination of cisplatin are 0.2 μM and 0.01316μA/μM, respectively. Furthermore, for determination of the linear range of the cisplatin sensor, the DPV measurements were also carried out for successive addition of 100 μM cisplatin solution, and the obtained calibration plot is presented in Figure 7, which illustrates that the linear range for determination of cisplatin on poly(cyc)/Ag-GO/GCE is 40-1200 μM. In addition, the obtained sensing results of the poly(cyc)/Ag-GO/GCE were compared with previously reported cisplatin sensors in Table 1, which illustrated that the linear range is considerably wider than other reported cisplatin sensors [54], synergetic effect of high chemical and mechanical stability of GO

and Ag nanoparticles [54], and effective role of electrodeposition and electropolymerization methods for in providing a stable sensing platform [55, 56].
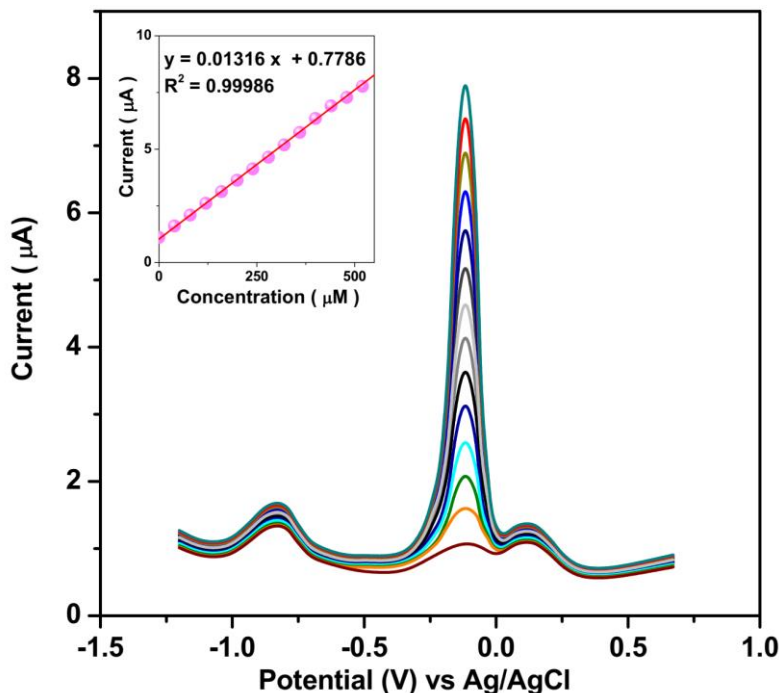

Figure 6. (a) DPV responses and (b) obtained calibration plots of poly(cyc)/Ag-GO/GCE in 0.1M PBS (pH=7.5) at 10mV/s scan rate to successive addition of 40 µM cisplatin.
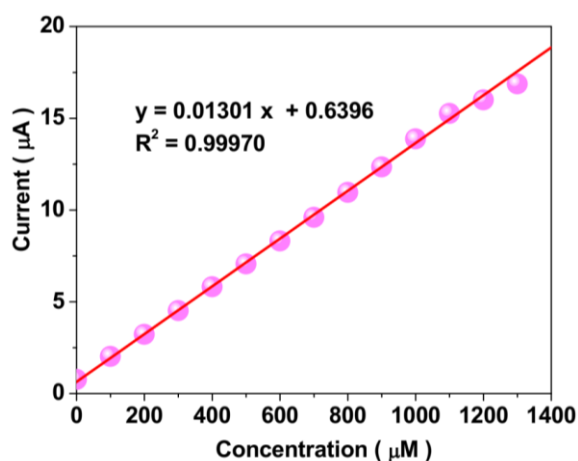

Figure 7. The obtained calibration plot of poly(cyc)/Ag-GO/GCE in 0.1M PBS (pH=7.5) at 10mV/s scan rate to successive addition of 100 µM cisplatin.

The selectivity of poly(cyc)/Ag-GO/GCE for determination of cisplatin was also investigated using DPV measurements in 0.1M PBS (pH=7.5) at a 10mV/s scan rate. Table 2 shows the results of DPV peak currents at -0.1V for modified electrodes in addition 50µM cisplatin and 150µM of some common species in biological fluids and pharmaceutical substances such as Al^{3+}, Fe^{3+}, Ca^{2+}, Li^+, Mg^{2+}, Na^+, Cu^{2+}, K^+, PO_4^{2-}, CO_3^{2-}, SO_4^{2-}, Cl^-, NO_3^-, dopamine, glucose, and ascorbic acid.

Table 1. Comparison the obtained sensing results of the poly(cyc)/Ag-GO/GCE with previously reported cisplatin sensors.

Electrodes	Technique	Detection limit (nM)	Linear range (μM)	Ref.
poly(cyc)/Ag-GO/GCE	DPV	0.2	40–1200	This work
MWCNT-COOH/ Screen printed electrode	DPV	4.6 μM	14.5-100	[22]
Metallothionein/ Hanging mercury drop electrode	DPV	0.5 μM	25–375	[23]
Graphene quantum dots-thionine/nano-porous glassy carbon electrode	DPV	0.09 μM	0.2-110	[24]
GO-MWNTs/GCE	CV	0.192 μM	1.3-26	[25]
GCE	CV	39.0 μM	65.4-303	[26]
dsDNA/rGO/GCE	AdTSV	0.3 μM	1–250	[57]

AdTSV: Adsorptive transfer stripping voltammetry

Table 2. Results of DPV responses of poly(cyc)/Ag-GO/GCE to addition 50 μM of cisplatin and 150 μM of some common species in biological fluids and pharmaceutical substances in 0.1M PBS (pH=7.5) in 10mV/s scan rate.

Specie	Concentration (μM)	DPV peak current at -0.1 V (μA)	RSD (%)
cisplatin	50	0.6548	±0.0149
Al^{3+}	150	0.0118	±0.0011
Fe^{3+}	150	0.0241	±0.0020
Ca^{2+}	150	0.0101	±0.0012
Li^+	150	0.0548	±0.0025
Mg^{2+}	150	0.0771	±0.0029
Na^+	150	0.0141	±0.0010
Cu^{2+}	150	0.0310	±0.0011
K^+	150	0.0182	±0.0017
PO_4^{2-}	150	0.0098	±0.0005
CO_3^{2-}	150	0.0099	±0.0010
SO_4^{2-}	150	0.0111	±0.0014
Cl^-	150	0.0257	±0.0032
NO_3^-	150	0.0320	±0.0028
Dopamine	150	0.0200	±0.0025
Glucose	150	0.0173	±0.0015
Ascorbic acid	150	0.0071	±0.0007

As observed, significant signals are obtained for the addition of cisplatin, indicating the sensitive response of the proposed cisplatin sensor, and the resultant weak and ignorable

electrocatalytic currents for successive addition substances are evidenced by the selective response of poly(cyc)/Ag-GO/GCE for the determination of cisplatin.
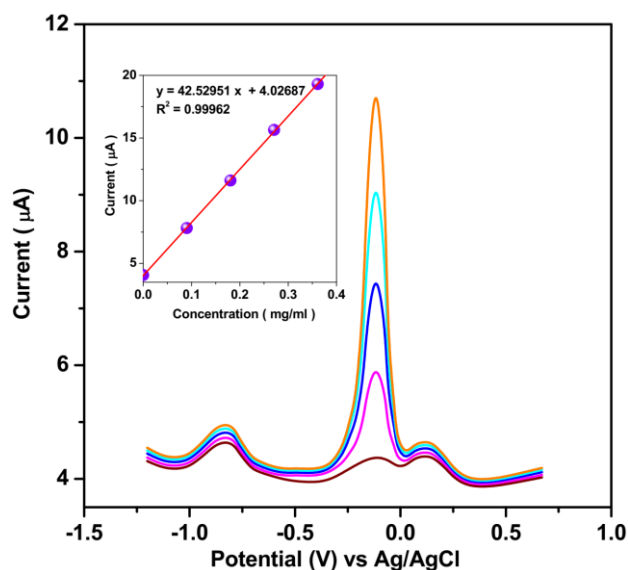

Figure 8. The DPV responses and obtained calibration plot of poly(cyc)/Ag-GO/GCE for determination the cisplatin concentration in prepared real specimen of platinol injection in 0.1M PBS (pH=7.5) in 10mV/s scan rate of in successive addition of cisplatin solution.

Table 3. Results of analytical studies for prepared real samples of platinol injection and cisplatin-free-human serum.

Sample	Added (mg/ml)	Found (mg/ml)	Recovery (%)	RSD (%)
Platinol injection	0.000	0.095	-	-
	0.100	0.192	97.00	3.08
	0.200	0.290	97.50	3.35
	0.300	0.388	97.66	4.57
	0.400	0.489	98.50	3.98
Human serum	0.000	0.000	-	-
	0.100	0.096	96.00	3.20
	0.200	0.194	97.00	3.75
	0.300	0.291	97.00	4.38
	0.400	0.381	95.25	4.76

The capability of the sensor was evaluated in prepared pharmaceutical and human serum real samples. Figure 8 shows the DPV responses and attained calibration plot of poly(cyc)/Ag-GO/GCE for determination of the cisplatin concentration in the prepared real sample of platinol injection in successive additions of cisplatin solution. The attained calibration plot shows the cisplatin content in the prepared platinol sample is 0.095 mg/ml that is very close to the cisplatin content of the platinol injection. Furthermore, Table 3 presents the results of analytical studies for prepared real specimens of

platinol injection and human serum. As observed, the ranges of recovery (95.25% to 98.50%) and RSD (3.08% to 4.76%) are acceptable and it is implied that the appropriate accuracy of the proposed cisplatin sensor for analyses of clinical specimens.

In order to further clinical investigation, the DPV and HPLC-MS measurements were carried out for the determination of the cisplatin content in urine samples of five patients aged 64 to 72 years with laryngeal cancer who underwent platinol injection treatment. Table 4 exhibits the results of an average of five determinations of cisplatin for each sample through the HPLC-MS technique and DPV measurements using poly(cyc)/Ag-GO/GCE. The comparison between the obtained results showed that there was good agreement between the HPLC-MS technique and DPV measurements on dsDNA/Au/GCE, and RSD (≤4.87%) values indicating the high accuracy of both techniques.

Table 4. Results of determinations of cisplatin content in urine of five patients aged 64 to 72 years with laryngeal cancer who underwent platinol injection treatment through HPLC-MS technique and DPV measurements using poly(cyc)/Ag-GO/GCE.

Sample	Cisplatin content in prepared real of urine (mg/ml)			
	poly(cyc)/Ag-GO/GCE	RSD (%)	HPLC-MS	RSD (%)
S1	459.01	±3.33	471.32	±4.02
S2	110.12	±2.79	123.54	±4.11
S3	359.24	±4.87	368.25	±3.87
S4	231.41	±3.13	221.27	±2.89
S5	222.09	±3.78	232.58	±3.58

4. CONCULUSION

This study was conducted on synthesis of poly(cyc)/Ag-GO/GCE for electrochemical monitoring of cisplatin. The Ag-GO composite was electrodeposied on GCE, and an electropolymerization method was applied for modification of the Ag-GO/GCE with poly(cyc). The results of structural studies of the Ag-GO composite showed that the Ag nanoparticles were discretely distributed on the surface of the GO nanosheets which provide a highly porous structure with the discrete electroactive sites for strong bonds of cyanocobalamin. Results of electrochemical analyses indicated a stable, sensitive and selective response of poly(cyc)/Ag-GO/GCE to the determination of cisplatin. The proposed sensor's detection limit, sensitivity, and linear range were determined to be 0.2μM, 0.01316μA/μM, and 40-1200μM, respectively. Results of investigation into the capability of the sensor in prepared real samples demonstrated acceptable ranges of recovery and RSD were acceptable, implying appropriate accuracy of the proposed cisplatin sensor for analyses of clinical samples.

References

1. H. Karimi-Maleh, M.L. Yola, N. Atar, Y. Orooji, F. Karimi, P.S. Kumar, J. Rouhi and M. Baghayeri, *Journal of colloid and interface science*, 592 (2021) 174.
2. T.-H. Wang, S.-M. Hsia, Y.-H. Shih and T.-M. Shieh, *International journal of molecular sciences*, 18 (2017) 1210.
3. X. Tong, F. Zhang, B. Ji, M. Sheng and Y. Tang, *Advanced Materials*, 28 (2016) 9979.
4. S. Yang, Z. Li, K. Yan, X. Zhang, Z. Xu, W. Liu, Z. Liu and H. Liu, *Journal of Environmental Sciences*, 103 (2021) 59.
5. M. Sakthivadivel, A. Nirmala, J. Sakthivadivel, R.R. Mukhilan and S. Tennyson, *Water Conservation & Management (WCM)*, 4 (2020) 90.
6. Y. Xie, X. Meng, D. Mao, Z. Qin, L. Wan and Y. Huang, *ACS Applied Materials & Interfaces*, 13 (2021) 32161.
7. B. Ji, F. Zhang, X. Song and Y. Tang, *Advanced materials*, 29 (2017)
8. X. Zhang, Y. Tang, F. Zhang and C.S. Lee, *Advanced Energy Materials*, 6 (2016) 1502588.
9. Y. Orooji, B. Tanhaei, A. Ayati, S.H. Tabrizi, M. Alizadeh, F.F. Bamoharram, F. Karimi, S. Salmanpour, J. Rouhi and S. Afshar, *Chemosphere*, 281 (2021) 130795.
10. K.A. Price and E.E. Cohen, *Current treatment options in oncology*, 13 (2012) 35.
11. Y. Tao, C. Ma, X. Yin, X. Fang and L. Liu, *Pakistan journal of medical sciences*, 32 (2016) 1126.
12. H. Karimi-Maleh, Y. Orooji, F. Karimi, M. Alizadeh, M. Baghayeri, J. Rouhi, S. Tajik, H. Beitollahi, S. Agarwal and V.K. Gupta, *Biosensors and Bioelectronics*, 184 (2021) 113252.
13. M. Eyankware, *Water Conservation and Management*, 3 (2019) 1.
14. Y. Orooji, P.N. Asrami, H. Beitollahi, S. Tajik, M. Alizadeh, S. Salmanpour, M. Baghayeri, J. Rouhi, A.L. Sanati and F. Karimi, *Journal of Food Measurement and Characterization*, (2021) 1.
15. Y. Sedletska, M.-J. Giraud-Panis and J.-M. Malinge, *Current Medicinal Chemistry-Anti-Cancer Agents*, 5 (2005) 251.
16. M. Van den Bent, W. Van Putten, P. Hilkens, R. de Wit and M. Van der Burg, *European Journal of Cancer*, 38 (2002) 387.
17. A. Lopez-Flores, R. Jurado and P. Garcia-Lopez, *Journal of pharmacological and toxicological methods*, 52 (2005) 366.
18. Z. Huang, A.R. Timerbaev, B.K. Keppler and T. Hirokawa, *Journal of Chromatography A*, 1106 (2006) 75.
19. D. Yaroshenko, A. Grigoriev, A. Sidorova and L. Kartsova, *Journal of Analytical Chemistry*, 68 (2013) 156.
20. B. Anilanmert, G. Yalçin, F. Ariöz and E. Dölen, *Analytical letters*, 34 (2001) 113.
21. S. Zalba, I. Navarro-Blasco, D. Moreno and M.J. Garrido, *Microchemical Journal*, 96 (2010) 415.
22. E.M. Materon, A. Wong, S.I. Klein, J. Liu and M.D.P.T. Sotomayor, *Electrochimica Acta*, 158 (2015) 271.
23. J. Petrlova, D. Potesil, J. Zehnalek, B. Sures, V. Adam, L. Trnkova and R. Kizek, *Electrochimica acta*, 51 (2006) 5169.
24. M.B. Gholivand, E. Ahmadi and M. Mavaei, *Sensors and Actuators B: Chemical*, 299 (2019) 126975.
25. L. Ye, M. Xiang, Y. Lu, Y. Gao and P. Pang, *International Journal of Electrochemical Science*, 9 (2014) 1537.
26. M.-l. Fang, Q.-l. Li, Q. Liu, Y.-x. Bei and Y.-t. Gao, *Chinese Journal of Pharmaceutical Analysis*, 31 (2011) 1165.

27. M. Shi, H. Zhu, C. Yang, J. Xu and C. Yan, *Chinese Journal of Chemical Engineering*, (2021) 1.
28. Z. Savari, S. Soltanian, A. Noorbakhsh, A. Salimi, M. Najafi and P. Servati, *Sensors and Actuators B: Chemical*, 176 (2013) 335.
29. H. Savaloni, E. Khani, R. Savari, F. Chahshouri and F. Placido, *Applied Physics A*, 127 (2021) 1.
30. X. Gao, R. Gui, K.Q. Xu, H. Guo, H. Jin and Z. Wang, *New Journal of Chemistry*, 42 (2018) 14796.
31. Y. Wang and Z.-z. Chen, *Talanta*, 82 (2010) 534.
32. A. Gerina-Berzina, S. Hasnere, A. Kolesovs, S. Umbrashko, R. Muceniece and I. Nakurte, *Exp Oncol*, 39 (2017) 124.
33. R.L. Whitby, *ACS nano*, 8 (2014) 9733.
34. R. Savari, J. Rouhi, O. Fakhar, S. Kakooei, D. Pourzadeh, O. Jahanbakhsh and S. Shojaei, *Ceramics International*, 47 (2021) 31927.
35. Y.-M. Fang, Z.-B. Lin, Y.-M. Zeng, W.-K. Chen, G.-N. Chen, J.-J. Sun, B. Ren and Z.-Q. Tian, *Chemistry-a European Journal*, 16 (2010) 6766.
36. H. Savaloni and R. Savari, *Materials Chemistry and Physics*, 214 (2018) 402.
37. R. Savari, H. Savaloni, S. Abbasi and F. Placido, *Sensors and Actuators B: Chemical*, 266 (2018) 620.
38. M. Vázquez, J. López, D. Medina-Rodelo, M. Jiménez-Edeza, G. Castañeda-Ruelas, A. López, J. Herrera-Ramírez and P. Méndez, *International Journal of Electrochemical Science*, 14 (2019) 6366.
39. Y. Lu, F. Yang, G.G. Wang, T. Zhang and P. Wang, *International Journal of Electrochemical Science*, 14 (2019) 5961.
40. C. Wang, X. Zhu, L. Zhang, Q. Song, H. Xu and X. Liu, *International Journal of Electrochemical Science*, 16 (2021) 210435.
41. W. Ali, V. Shabani, M. Linke, S. Sayin, B. Gebert, S. Altinpinar, M. Hildebrandt, J.S. Gutmann and T. Mayer-Gall, *RSC advances*, 9 (2019) 4553.
42. D. Tonelli, E. Scavetta and I. Gualandi, *Sensors*, 19 (2019) 1186.
43. N. Yang, Q. Wan and X. Wang, *Electrochimica acta*, 50 (2005) 2175.
44. Y. Zheng, Y. Li and Z. Deng, *Chemical Communications*, 48 (2012) 6160.
45. A.M. de Medeiros, L.U. Khan, G.H. da Silva, C.A. Ospina, O.L. Alves, V.L. de Castro and D.S.T. Martinez, *Ecotoxicology and Environmental Safety*, 209 (2021) 111776.
46. I.H. Lambert and B.H. Sørensen, *International journal of molecular sciences*, 19 (2018) 2249.
47. D. Corinti, C. Coletti, N. Re, S. Piccirillo, M. Giampa, M.E. Crestoni and S. Fornarini, *RSC advances*, 7 (2017) 15877.
48. A. Melchior, M. Tolazzi, J.M. Martínez, R.R. Pappalardo and E. Sanchez Marcos, *Journal of chemical theory and computation*, 11 (2015) 1735.
49. S. Ahmed, M. Ahmad, B.L. Swami and S. Ikram, *Journal of advanced research*, 7 (2016) 17.
50. X. Ran, Y. Du, Z. Wang, H. Wang, F. Pu, J. Ren and X. Qu, *ACS applied materials & interfaces*, 9 (2017) 19717.
51. N. Thepphankulngarm, P. Wonganan, C. Sapcharoenkun, T. Tuntulani and P. Leeladee, *New Journal of Chemistry*, 41 (2017) 13823.
52. H. Savaloni, R. Savari and S. Abbasi, *Current Applied Physics*, 18 (2018) 869.
53. F. Chahshouri, H. Savaloni, E. Khani and R. Savari, *Journal of Micromechanics and Microengineering*, 30 (2020) 075001.
54. T.T.T. Vi, S. Rajesh Kumar, B. Rout, C.-H. Liu, C.-B. Wong, C.-W. Chang, C.-H. Chen, D.W. Chen and S.J. Lue, *Nanomaterials*, 8 (2018) 163.
55. B. Lakard, G. Herlem, S. Lakard, R. Guyetant and B. Fahys, *Polymer*, 46 (2005) 12233.
56. R. Dasari and F.P. Zamborini, *Journal of the American Chemical Society*, 130 (2008) 16138.

57.   Y. Yardım, M. Vandeput, M. Çelebi, Z. Şentürk and J.M. Kauffmann, *Electroanalysis*, 29 (2017) 1451.